

Article

A COVID-19 Infection Model Considering the Factors of Environmental Vectors and Re-Positives and Its Application to Data Fitting in Japan and Italy

Shimeng Dong¹, Jinlong Lv¹, Wanbiao Ma^{1,*}  and Boralahala Gamage Sampath Aruna Pradeep² 

¹ Department of Applied Mathematics, School of Mathematics and Physics, University of Science and Technology Beijing, Beijing 100083, China

² Department of Mathematics, University of Ruhuna, Matara 81000, Sri Lanka

* Correspondence: wanbiao_ma@ustb.edu.cn

Abstract: COVID-19, which broke out globally in 2019, is an infectious disease caused by a novel strain of coronavirus, and its spread is highly contagious and concealed. Environmental vectors play an important role in viral infection and transmission, which brings new difficulties and challenges to disease prevention and control. In this paper, a type of differential equation model is constructed according to the spreading functions and characteristics of exposed individuals and environmental vectors during the virus infection process. In the proposed model, five compartments were considered, namely, susceptible individuals, exposed individuals, infected individuals, recovered individuals, and environmental vectors (contaminated with free virus particles). In particular, the re-positive factor was taken into account (i.e., recovered individuals who have lost sufficient immune protection may still return to the exposed class). With the basic reproduction number \mathcal{R}_0 of the model, the global stability of the disease-free equilibrium and uniform persistence of the model were completely analyzed. Furthermore, sufficient conditions for the global stability of the endemic equilibrium of the model were also given. Finally, the effective predictability of the model was tested by fitting COVID-19 data from Japan and Italy.

Keywords: COVID-19 infection; asymptomatic infection/re-positive; environmental vector; stability; data fitting



Citation: Dong, S.; Lv, J.; Ma, W.; Pradeep, B.G.S.A. A COVID-19 Infection Model Considering the Factors of Environmental Vectors and Re-Positives and Its Application to Data Fitting in Japan and Italy. *Viruses* **2023**, *15*, 1201. <https://doi.org/10.3390/v15051201>

Academic Editors: Thanasis Fokas and George Kastis

Received: 5 February 2023

Revised: 10 May 2023

Accepted: 10 May 2023

Published: 19 May 2023



Copyright: © 2023 by the authors. Licensee MDPI, Basel, Switzerland. This article is an open access article distributed under the terms and conditions of the Creative Commons Attribution (CC BY) license (<https://creativecommons.org/licenses/by/4.0/>).

1. Introduction

In 2019, an unexplained novel coronavirus disease (COVID-19) suddenly broke out, which triggered an unprecedented public health crisis in the world. On 11 March 2020, the World Health Organization (WHO) declared COVID-19 as a global pandemic. COVID-19 is caused by a novel coronavirus named severe acute respiratory syndrome coronavirus 2 (SARS-CoV-2) [1]. SARS-CoV-2 is regarded as the third zoonotic coronavirus emerging in the current century, after SARS-CoV in 2002 and the Middle East respiratory syndrome coronavirus (MERS-CoV) in 2012 [2,3]. Common signs of COVID-19 infection include respiratory symptoms, fever, cough, shortness of breath, and difficulty of breathing, and in more serious cases, it can lead to pneumonia, severe acute respiratory syndrome, renal failure, and even death due to alveolar damage, posing a serious threat to human life [4,5]. Among the low-risk people who died of COVID-19, 70% of them had one or more organ dysfunctions within 4 months of the initial symptoms of COVID-19, and experienced organ damage, fatigue, muscle weakness, difficulty of sleeping, anxiety, or depression after the acute phase [6,7]. On a global scale, as of 24 May 2022, countries around the world have reported more than 500 million confirmed cases of COVID-19 to the WHO, including 6.2 million deaths cases [8].

It is encouraging that in the past two years, with the joint efforts of scientists from many countries, a series of important research achievements have been made in the field of

drugs for COVID-19 treatment, improving the effectiveness of vaccines, which have greatly contributed to protecting people’s health and lives [9,10].

In particular, differential equations and statistics have been widely used to construct various types of compartmental models and make rapid and effective predictions about infection trends, epidemic patterns, and key factors in the spread of infectious diseases. In addition, mathematical models based on differential equations provide a theoretical basis and optimal strategies for the prevention and treatment of infectious diseases [11–27].

It is known that environmental vectors play an important role in virus infection and transmission, and bring new difficulties and challenges to the prevention and control of the disease. For example, a study reviewing 22 types of coronaviruses revealed that viruses such as SARS-CoV, SARS-CoV, MERS-CoV, and endemic human coronaviruses can persist for up to 9 days on inanimate surfaces such as metal, glass, or plastic [28]. Another experimental study found that SARS-CoV-2 can be detected on aerosols for up to 3 h, on copper for up to 4 h, on cardboard for up to 24 h, and on plastic and stainless steel for up to 3 days [29]. Moreover, SARS-CoV-2 can also be detected in domestic wastewater [30,31]. In recent years, many scholars have conducted extensive research on infectious disease models with media effects [32–40]. In addition, many scholars have considered the possible factor of re-positives and designed a new model based on the traditional SEIR-type to analyze the spread of the epidemic [41,42], which can also be seen in previous studies [43–50]. According to previous studies, re-positives and environmental vectors significantly impact COVID-19 dynamics and evolution, and need to be investigated widely in order to uncover the strength of disease severity and infectiousness. It has not yet been extensively explored using mathematical modeling studies. Therefore, it is necessary to use differential equation modeling methods to help understand the mechanism of environmental vectors and re-positive factors in virus transmission.

The authors of [41] consider the situation of re-infection, where recovered people may return to being considered infected people (including symptomatic and asymptomatic infected people), and these infected people can release virus particles into the environment. In order to simplify the model, we let exposed people to include lurkers and asymptomatic infected people. We assume that asymptomatic infected people are infectious, and that all infected people must undergo the incubation period.

In addition to the factors mentioned in [41], the following three types of factors are also considered: the first is that exposed individuals are still contagious, and exposed individuals can transmit viruses deposited on the surface of materials to healthy individuals through inanimate substances (public lift buttons, mail packages, etc.); the second is that the birth population is not zero, the mortality rate of different populations is also different, and recovered individuals may return to becoming susceptible individuals due to immune loss; the third is that we consider the recovered of re-positives to return to becoming exposed people.

Let the variables $S(t)$, $E(t)$, $I(t)$, and $R(t)$ represent the numbers of susceptible individuals, exposed individuals, infected individuals, and recovered individuals at time t , respectively, and $M(t)$ represent the number of free virus particles accumulated in environmental vectors. The block diagram of the interactions among S , E , I , R , and M is shown below (Figure 1).

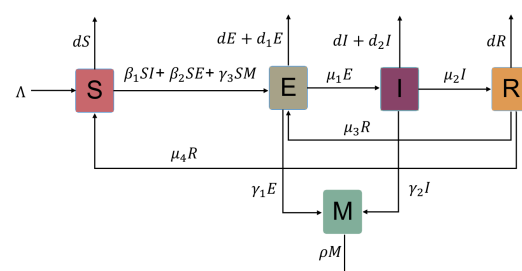


Figure 1. The block diagram of the interactions among S , E , I , R , and M .

According to the above block diagram of the interaction between these state variables, we have the following five-dimensional ordinary differential equation model:

$$\begin{cases} \dot{S}(t) = \Lambda - \beta_1 S(t)I(t) - \beta_2 S(t)E(t) - \gamma_3 S(t)M(t) + \mu_4 R(t) - dS(t), \\ \dot{E}(t) = \beta_1 S(t)I(t) + \beta_2 S(t)E(t) + \gamma_3 S(t)M(t) + \mu_3 R(t) - (d + d_1 + \mu_1)E(t), \\ \dot{I}(t) = \mu_1 E(t) - (d + d_2 + \mu_2)I(t), \\ \dot{R}(t) = \mu_2 I(t) - (d + \mu_3 + \mu_4)R(t), \\ \dot{M}(t) = \gamma_1 E(t) + \gamma_2 I(t) - \rho M(t). \end{cases} \quad (1)$$

The biological meanings of each parameter in model (1) are shown in Table 1 below:

Table 1. Biological meanings of the parameters in model (1.1).

| Parameter | Description | Unit |
|------------|---|--|
| β_1 | Infection rate of infected individuals | /10,000 persons \times day |
| β_2 | Infection rate of exposed individuals | /10,000 persons \times day |
| γ_1 | Rate of virus release into the environment by exposed individuals | 10,000 viruses/10,000 persons \times day |
| γ_2 | Rate of virus release into the environment by infected individuals | 10,000 viruses/10,000 persons \times day |
| γ_3 | Infection rate due to environmental vectors | /10,000 viruses \times day |
| ρ | Rate of decay or clearance of free virus particles in environmental vectors | /day |
| Λ | Population input rate | 10,000 persons/day |
| μ_1 | Rate at which exposed individuals become infected | /day |
| μ_2 | Recovery rate of infected people | /day |
| μ_3 | Rate of re-positives | /day |
| μ_4 | Rate at which recovered individuals without immune protection return to the susceptible class | /day |
| d | Natural death rate | /day |
| d_1 | Death rate of exposed individuals caused by virus | /day |
| d_2 | Death rate of infected individuals caused by virus | /day |

Considering the biological meaning, all the parameters in Table 1 are non-negative constants, $\Lambda > 0$, $d > 0$, and $\rho > 0$.

The main purpose of the paper can be divided into two parts. Firstly, the local and global stability of the equilibria and uniform persistence of model (1) are analyzed in detail by using the basic reproduction number. Secondly, model (1) is applied to data fitting of COVID-19 from Japan and Italy, which shows the effectiveness and predictability of the model. Furthermore, the paper conducts a sensitivity analysis of the parameters in model (1) using data from Italy, which allows us to identify the main factors related to disease transmission (for example, the infection rate of infected individuals (β_1), infection rate of exposed individuals (β_2), rate of virus release into the environment by infected individuals (γ_2), infection rate due to environmental vectors (γ_3), rate of decay or clearance of free virus particles in environmental vectors (ρ), rate at which exposed individuals become infected (μ_1), recovery rate of infected people (μ_2), rate of re-positives (μ_3), and the rate at which recovered individuals without immune protection return to the susceptible class (μ_4)).

2. Stability and Uniform Persistence

The initial condition of model (1) is

$$S(0) = S^0, E(0) = E^0, I(0) = I^0, R(0) = R^0, M(0) = M^0, \quad (2)$$

where S^0, E^0, I^0, R^0 , and M^0 are non-negative constants.

It is easy to prove that the solution $(S(t), E(t), I(t), R(t), M(t))$ of model (1) with the initial condition (2) is existent, unique, non-negative, and ultimately bounded in $[0, +\infty)$, and satisfies

$$\limsup_{t \rightarrow \infty} (S(t) + E(t) + I(t) + R(t)) \leq \Lambda d^{-1}, \quad \limsup_{t \rightarrow \infty} M(t) \leq (\gamma_1 + \gamma_2)\Lambda(d\rho)^{-1}.$$

2.1. Basic Reproduction Number and Classification of Equilibria

Model (1) always has the disease-free equilibrium $Q_0 = (S_0, 0, 0, 0, 0)$, where $S_0 = \Lambda d^{-1}$. By the method of the next generation matrix [51,52], we obtain the basic reproduction number of model (1), as follows:

$$\mathcal{R}_0 = \rho(FV^{-1}) = \frac{\Lambda(d + \mu_3 + \mu_4)[(\rho\beta_2 + \gamma_1\gamma_3)(d + d_2 + \mu_2) + \mu_1(\rho\beta_1 + \gamma_2\gamma_3)]}{d\rho[(d + d_1 + \mu_1)(d + d_2 + \mu_2)(d + \mu_3 + \mu_4) - \mu_1\mu_2\mu_3]}.$$

where

$$F = \begin{bmatrix} \frac{\beta_2\Lambda}{d} & \frac{\beta_1\Lambda}{d} & 0 & \frac{\gamma_3\Lambda}{d} \\ 0 & 0 & 0 & 0 \\ 0 & 0 & 0 & 0 \\ 0 & 0 & 0 & 0 \end{bmatrix}, \quad V = \begin{bmatrix} d + d_1 + \mu_1 & 0 & -\mu_3 & 0 \\ -\mu_1 & d + d_2 + \mu_2 & 0 & 0 \\ 0 & -\mu_2 & d + \mu_3 + \mu_4 & 0 \\ -\gamma_1 & -\gamma_2 & 0 & \rho \end{bmatrix}.$$

It is not difficult to see that \mathcal{R}_0 can be written as $\mathcal{R}_0 = \mathcal{R}_1 + \mathcal{R}_2 + \mathcal{R}_3$, where

$$\begin{aligned} \mathcal{R}_1 &= \frac{\mu_1(d + \mu_3 + \mu_4)\beta_1 S_0}{(d + d_1 + \mu_1)(d + d_2 + \mu_2)(d + \mu_3 + \mu_4) - \mu_1\mu_2\mu_3}, \\ \mathcal{R}_2 &= \frac{(d + d_2 + \mu_2)(d + \mu_3 + \mu_4)\beta_2 S_0}{(d + d_1 + \mu_1)(d + d_2 + \mu_2)(d + \mu_3 + \mu_4) - \mu_1\mu_2\mu_3}, \\ \mathcal{R}_3 &= \frac{[\mu_1\gamma_2 + \gamma_1(d + d_2 + \mu_2)](d + \mu_3 + \mu_4)\gamma_3 S_0}{\rho[(d + d_1 + \mu_1)(d + d_2 + \mu_2)(d + \mu_3 + \mu_4) - \mu_1\mu_2\mu_3]}. \end{aligned}$$

According to the expressions of $\mathcal{R}_1, \mathcal{R}_2$, and \mathcal{R}_3 , it can be clearly seen that the value of the basic reproduction number \mathcal{R}_0 directly depends on the infection rate of the infected individuals (β_1), the infection rate of exposed individuals (β_2), and the infection rate due to environmental vectors (γ_3).

Assuming that (S, E, I, R, M) can be any equilibrium of model (1), it has the following equations:

$$\begin{cases} \Lambda - \beta_1 SI - \beta_2 SE - \gamma_3 SM + \mu_4 R - dS = 0, \\ \beta_1 SI + \beta_2 SE + \gamma_3 SM + \mu_3 R - (d + d_1 + \mu_1)E = 0, \\ \mu_1 E - (d + d_2 + \mu_2)I = 0, \\ \mu_2 I - (d + \mu_3 + \mu_4)R = 0, \\ \gamma_1 E + \gamma_2 I - \rho M = 0. \end{cases} \tag{3}$$

By solving the equations (3), it is easy to obtain that when $\mathcal{R}_0 > 1$, model (1) has a unique endemic equilibrium $Q^* = (S^*, E^*, I^*, R^*, M^*)$, where

$$\begin{aligned} S^* &= \frac{\rho(d + d_1 + \mu_1)(d + d_2 + \mu_2)(d + \mu_3 + \mu_4) - \rho\mu_1\mu_2\mu_3}{\mu_1(\rho\beta_1 + \gamma_2\gamma_3)(d + \mu_3 + \mu_4) + (\rho\beta_2 + \gamma_1\gamma_3)(d + d_2 + \mu_2)(d + \mu_3 + \mu_4)} = \frac{\Lambda}{\mathcal{R}_0 d}, \\ E^* &= \frac{(d + d_2 + \mu_2)(d + \mu_3 + \mu_4)}{\mu_1\mu_2} R^*, \quad I^* = \frac{(d + \mu_3 + \mu_4)}{\mu_2} R^*, \\ R^* &= \left(1 - \frac{1}{\mathcal{R}_0}\right) \frac{\mu_1\mu_2\Lambda}{(d + d_1 + \mu_1)(d + d_2 + \mu_2)(d + \mu_3 + \mu_4) - (\mu_1\mu_2\mu_3 + \mu_1\mu_2\mu_4)}, \\ M^* &= \frac{\gamma_1(d + d_2 + \mu_2)(d + \mu_3 + \mu_4) + \mu_1\gamma_2(d + \mu_3 + \mu_4)}{\mu_1\mu_2\rho} R^*. \end{aligned}$$

2.2. Global Stability of the Disease-Free Equilibrium

It is clear that the set

$$\Omega = \left\{ (E, I, R, M) \mid E, I, R, M \geq 0, S + E + I + R \leq S_0, M \leq (\gamma_1 + \gamma_2)\Lambda(d\rho)^{-1} \right\}$$

is attractive and positively invariant with respect to model (1). Thus, this leads to the following theorem:

Theorem 1. *If $\mathcal{R}_0 < 1$, the disease-free equilibrium Q_0 of model (1) is globally asymptotically stable with respect to Ω .*

Proof. Firstly, let us show that the disease-free equilibrium Q_0 is locally asymptotically stable. For convenience, let $d + d_1 + \mu_1 = a_1$, $d + d_2 + \mu_2 = a_2$, and $d + \mu_3 + \mu_4 = a_3$. Hence, $a_1 a_2 a_3 - \mu_1 \mu_2 \mu_3 > 0$.

Using simple calculations, we can determine that the characteristic equation of model (1) at the disease-free equilibrium Q_0 is $(\lambda + d)g(\lambda) = 0$, where

$$g(\lambda) = -\frac{\gamma_3 \Lambda}{d}(\lambda + a_3)[\mu_1 \gamma_2 + \gamma_1(\lambda + a_2)] + (\lambda + \rho)\left(\lambda - \frac{\beta_2 \Lambda}{d} + a_1\right)(\lambda + a_2)(\lambda + a_3) - (\lambda + \rho)\left[\frac{\mu_1 \beta_1 \Lambda}{d}(\lambda + a_3) + \mu_1 \mu_2 \mu_3\right].$$

Clearly, $\lambda_1 = -d$ is a negative root. Let us further show that when $\mathcal{R}_0 < 1$, all the roots of the equation $g(\lambda) = 0$ have negative real parts. Suppose that $\lambda = x + iy$ ($x \geq 0$) is an eigenvalue of the equation $g(\lambda) = 0$.

Then, the equation $g(\lambda) = 0$ can be rewritten in the following equivalent form:

$$1 = \frac{\mu_1 \gamma_2 \gamma_3 \Lambda}{d(\lambda + \rho)(\lambda + a_1)(\lambda + a_2)} + \frac{\gamma_1 \gamma_3 \Lambda}{d(\lambda + \rho)(\lambda + a_1)} + \frac{\beta_2 \Lambda}{d(\lambda + a_1)} + \frac{\mu_1 \beta_1 \Lambda}{d(\lambda + a_1)(\lambda + a_2)} + \frac{\mu_1 \mu_2 \mu_3}{(\lambda + a_1)(\lambda + a_2)(\lambda + a_3)}.$$

Taking the modulus on both sides of the above equality, it becomes

$$\begin{aligned} 1 &= \left| \frac{\mu_1 \gamma_2 \gamma_3 \Lambda}{d(\lambda + \rho)(\lambda + a_1)(\lambda + a_2)} + \frac{\gamma_1 \gamma_3 \Lambda}{d(\lambda + \rho)(\lambda + a_1)} + \frac{\beta_2 \Lambda}{d(\lambda + a_1)} + \frac{\mu_1 \beta_1 \Lambda}{d(\lambda + a_1)(\lambda + a_2)} \right. \\ &\quad \left. + \frac{\mu_1 \mu_2 \mu_3}{(\lambda + a_1)(\lambda + a_2)(\lambda + a_3)} \right| \\ &\leq \left| \frac{\mu_1 \gamma_2 \gamma_3 \Lambda}{d(\lambda + \rho)(\lambda + a_1)(\lambda + a_2)} \right| + \left| \frac{\gamma_1 \gamma_3 \Lambda}{d(\lambda + \rho)(\lambda + a_1)} \right| + \left| \frac{\beta_2 \Lambda}{d(\lambda + a_1)} \right| + \left| \frac{\mu_1 \beta_1 \Lambda}{d(\lambda + a_1)(\lambda + a_2)} \right| \\ &\quad + \left| \frac{\mu_1 \mu_2 \mu_3}{(\lambda + a_1)(\lambda + a_2)(\lambda + a_3)} \right| \\ &\leq \frac{\mu_1 \gamma_2 \gamma_3 \Lambda}{d\rho a_1 a_2} + \frac{\gamma_1 \gamma_3 a_2 \Lambda}{d\rho a_1 a_2} + \frac{\beta_2 \rho a_2 \Lambda}{d\rho a_1 a_2} + \frac{\mu_1 \beta_1 \rho \Lambda}{d\rho a_1 a_2} + \frac{\mu_1 \mu_2 \mu_3}{a_1 a_2 a_3} \\ &= \frac{\Lambda(\mu_1 \gamma_2 \gamma_3 + \mu_1 \beta_1 \rho + \gamma_1 \gamma_3 a_2 + \beta_2 \rho a_2)}{d\rho a_1 a_2} + \frac{\mu_1 \mu_2 \mu_3}{a_1 a_2 a_3} \\ &= \frac{(a_1 a_2 a_3 - \mu_1 \mu_2 \mu_3)}{a_1 a_2 a_3} \mathcal{R}_0 + \frac{\mu_1 \mu_2 \mu_3}{a_1 a_2 a_3} \\ &= \mathcal{R}_0 + (1 - \mathcal{R}_0) \frac{\mu_1 \mu_2 \mu_3}{a_1 a_2 a_3}. \end{aligned}$$

Note that $a_1 a_2 a_3 - \mu_1 \mu_2 \mu_3 > 0$ and $\mathcal{R}_0 < 1$, meaning that the above inequality is not valid. This proves that when $\mathcal{R}_0 < 1$, all the roots of the equation $g(\lambda) = 0$ have negative real parts. Hence, the disease-free equilibrium Q_0 is locally asymptotically stable.

Next, we show that the disease-free equilibrium Q_0 is globally attractable. In fact, for $t \geq 0$, model (1) implies

$$\begin{cases} \dot{E}(t) \leq \beta_1 S_0 I(t) + \beta_2 S_0 E(t) + \gamma_3 S_0 M(t) + \mu_3 R(t) - (d + d_1 + \mu_1)E(t), \\ \dot{I}(t) \leq \mu_1 E(t) - (d + d_2 + \mu_2)I(t), \\ \dot{R}(t) \leq \mu_2 I(t) - (d + \mu_3 + \mu_4)R(t), \\ \dot{M}(t) \leq \gamma_1 E(t) + \gamma_2 I(t) - \rho M(t). \end{cases}$$

Let $Y = (y_1, y_2, y_3, y_4)^T$, and consider the comparison system $\frac{dY}{dt} = (F - V)Y$. As the condition $\mathcal{R}_0 = \rho(FV^{-1}) < 1$ means that all eigenvalues of matrix $F - V$ have negative real parts, the trivial solution of the comparison system is asymptotically stable. Therefore, it follows that $E(t) \leq y_1(t) \rightarrow 0, I(t) \leq y_2(t) \rightarrow 0, R(t) \leq y_3(t) \rightarrow 0$ and $M(t) \leq y_4(t) \rightarrow 0$ for $t \rightarrow +\infty$. Furthermore, from the first equation of model (1), it is easy to obtain $S(t) \rightarrow S_0$ for $t \rightarrow +\infty$. This proves that the disease-free equilibrium Q_0 is globally attractive with respect to the set Ω . \square

2.3. Uniform Persistence and Global Stability of the Endemic Equilibrium

In the subsection, there is the following Theorem 2 for the uniform persistence of model (1).

Theorem 2. *If $\mathcal{R}_0 > 1$, then model (1) is uniformly persistent, and each positive solution $(S(t), E(t), I(t), R(t), M(t))^T$ of model (1) with the initial condition (2) satisfies*

$$\begin{aligned} \liminf_{t \rightarrow \infty} S(t) &\geq \frac{\Lambda d}{\Lambda[\beta_1 + \beta_2 + \gamma_3(\gamma_1 + \gamma_2)\rho^{-1}] + d^2} \equiv v_1, & \liminf_{t \rightarrow \infty} E(t) &\geq \delta E^* e^{-Ta_1} \equiv v_2, \\ \liminf_{t \rightarrow \infty} I(t) &\geq \frac{\mu_1}{a_2} v_2, & \liminf_{t \rightarrow \infty} R(t) &\geq \frac{\mu_1 \mu_2}{a_2 a_3} v_2, & \liminf_{t \rightarrow \infty} M(t) &\geq \left(\frac{\gamma_1}{\rho} + \frac{\gamma_2 \mu_1}{a_2 \rho} \right) v_2, \end{aligned}$$

where $\delta > 0$ and $T > 0$, and satisfies

$$q \equiv \left(\frac{\beta_1 v_2}{a_2} + \beta_2 + \frac{\gamma_1 \gamma_3}{\rho} + \frac{\gamma_2 \gamma_3 \mu_1}{a_2 \rho} \right) \delta E^* + d, \quad \frac{\Lambda}{q} > S^*, \quad S^\Delta \equiv \frac{\Lambda}{q} (1 - e^{-Tq}) > S^*.$$

To complete the proof of Theorem 2, the key point is to show that the estimation $\liminf_{t \rightarrow +\infty} E(t) \geq v_2$ holds. The detailed proof is similar to [53–56] and has been omitted here.

From a biological point of view, Theorem 2 indicates that as long as the basic reproduction number $\mathcal{R}_0 > 1$, the disease infection cannot be eliminated and will permanently exist.

Next, let us consider the global asymptotic stability of the endemic equilibrium Q^* of model (1). To simplify model (1), it is assumed that the death rate of the exposed and infected individuals caused by the virus is zero, i.e., (H1) $d_1 = d_2 = 0$.

Let $N(t) = S(t) + E(t) + I(t) + R(t)$, then for $t \geq 0$, we have $\dot{N}(t) = \Lambda - dN(t)$, which implies $\lim_{t \rightarrow +\infty} N(t) = S_0$. On the hyperplane $N = S_0$, model (1) can be transformed into the following equivalent four-dimensional system:

$$\begin{cases} \dot{S}(t) = \Lambda - \beta_1 S(t)I(t) - \beta_2 S(t)E(t) - \gamma_3 S(t)M(t) + \mu_4(S_0 - S(t) - E(t) - I(t)) - dS(t), \\ \dot{E}(t) = \beta_1 S(t)I(t) + \beta_2 S(t)E(t) + \gamma_3 S(t)M(t) + \mu_3(S_0 - S(t) - E(t) - I(t)) - (d + \mu_1)E(t), \\ \dot{I}(t) = \mu_1 E(t) - (d + \mu_2)I(t), \\ \dot{M}(t) = \gamma_1 E(t) + \gamma_2 I(t) - \rho M(t). \end{cases} \tag{4}$$

In addition, the following conditions are also used:

(H2) $\mu_2 + \mu_3 - 2\mu_1 - \mu_4 > 0, d + \mu_1 + \mu_3 - (2\beta_1 + 2\beta_2)S_0 - \rho - 2\mu_4 > 0, d + \mu_2 - \mu_1 > 0, \gamma_1 \geq \gamma_2, 2\mu_4 \geq \mu_1 + \mu_3.$

By using a similar method to what was used in [57–59], we have Theorem 3.

Theorem 3. *If the conditions (H1)–(H2) hold, then, when $\mathcal{R}_0 > 1$, the endemic equilibrium Q^* of system (4) is globally asymptotically stable with respect to Ω .*

Proof. For system (4), the Jacobian matrix J and second additive compound matrix $J^{[2]}$ are given by

$$J = \begin{pmatrix} -\beta_1 I - \beta_2 E - \gamma_3 M - d - \mu_4 & -\beta_2 S - \mu_4 & -\beta_1 S - \mu_4 & -\gamma_3 S \\ \beta_1 I + \beta_2 E + \gamma_3 M - \mu_3 & \beta_2 S - d - \mu_1 - \mu_3 & \beta_1 S - \mu_3 & \gamma_3 S \\ 0 & \mu_1 & -d - \mu_2 & 0 \\ 0 & \gamma_1 & \gamma_2 & -\rho \end{pmatrix}$$

and

$$J^{[2]} = \begin{pmatrix} M_{11} & \beta_1 S - \mu_3 & \gamma_3 S & \beta_1 S + \mu_4 & \gamma_3 S & 0 \\ \mu_1 & M_{22} & 0 & -\beta_2 S - \mu_4 & 0 & \gamma_3 S \\ \gamma_1 & \gamma_2 & M_{33} & 0 & -\beta_2 S - \mu_4 & -\beta_1 S - \mu_4 \\ 0 & q & 0 & M_{44} & 0 & -\gamma_3 S \\ 0 & 0 & q & \gamma_2 & M_{55} & \beta_1 S - \mu_3 \\ 0 & 0 & 0 & -\gamma_1 & \mu_1 & M_{66} \end{pmatrix},$$

where

$$\begin{aligned} M_{11} &= -\beta_1 I - \beta_2 E - \gamma_3 M - d - \mu_4 + \beta_2 S - d - \mu_1 - \mu_3, \\ M_{22} &= -\beta_1 I - \beta_2 E - \gamma_3 M - d - \mu_4 - d - \mu_2, \\ M_{33} &= -\beta_1 I - \beta_2 E - \gamma_3 M - d - \mu_4 - \rho, \\ M_{44} &= \beta_2 S - 2d - \mu_1 - \mu_3 - \mu_2, \\ M_{55} &= \beta_2 S - d - \mu_1 - \mu_3 - \rho, \\ M_{66} &= -d - \mu_2 - \rho, \\ q &= \beta_1 I + \beta_2 E + \gamma_3 M - \mu_3. \end{aligned}$$

Let

$$P = P(S, E, I, M) = \begin{pmatrix} \frac{1}{E} & 0 & 0 & 0 & 0 & 0 \\ 0 & \frac{1}{E} & 0 & 0 & 0 & 0 \\ 0 & 0 & 0 & \frac{1}{E} & 0 & 0 \\ 0 & 0 & \frac{1}{M} & 0 & 0 & 0 \\ 0 & 0 & 0 & 0 & \frac{1}{M} & 0 \\ 0 & 0 & 0 & 0 & 0 & \frac{1}{M} \end{pmatrix},$$

using f to represent the vector form of system (4). Then, P_f is the directional derivative of $P(x)$ along the direction of f . It follows that $P_f P^{-1} = \text{diag}\left\{-\frac{\dot{E}}{E}, -\frac{\dot{E}}{E}, -\frac{\dot{E}}{E}, -\frac{\dot{M}}{M}, -\frac{\dot{M}}{M}, -\frac{\dot{M}}{M}\right\}$, and

$$\begin{aligned} Q(S, E, I, M) &= P_f P^{-1} + P J^{[2]} P^{-1} \\ &= \begin{pmatrix} M_{11} - \frac{\dot{E}}{E} & \beta_1 S - \mu_3 & \beta_1 S + \mu_4 & \frac{\gamma_3 S M}{E} & \frac{\gamma_3 S M}{E} & 0 \\ \mu_1 & M_{22} - \frac{\dot{E}}{E} & -\beta_2 S - \mu_4 & 0 & 0 & \frac{\gamma_3 S M}{E} \\ 0 & q & M_{44} - \frac{\dot{E}}{E} & 0 & 0 & -\frac{\gamma_3 S M}{E} \\ \frac{\gamma_2 E}{M} & \frac{\gamma_2 E}{M} & 0 & M_{33} - \frac{\dot{M}}{M} & -\beta_2 S - \mu_4 & -\beta_1 S - \mu_4 \\ 0 & 0 & \frac{\gamma_2 E}{M} & q & M_{55} - \frac{\dot{M}}{M} & \beta_1 S - \mu_3 \\ 0 & 0 & -\frac{\gamma_1 E}{M} & 0 & \mu_1 & M_{55} - \frac{\dot{M}}{M} \end{pmatrix}. \end{aligned}$$

The matrix $Q(S, E, I, M)$ can be written in block form: $Q(S, E, I, M) = (Q_{ij})_{4 \times 4}$, where

$$\begin{aligned}
 Q_{11} &= M_{11} - \frac{\dot{E}}{E}, & Q_{12} &= (\beta_1 S - \mu_3, \beta_1 S + \mu_4), & Q_{13} &= \left(\frac{\gamma_3 SM}{E}, \frac{\gamma_3 SM}{E} \right), & Q_{14} &= 0, \\
 Q_{21} &= (\mu_1, 0)^T, & Q_{22} &= \begin{pmatrix} M_{22} - \frac{\dot{E}}{E} & -\beta_2 S - \mu_4 \\ q & M_{44} - \frac{\dot{E}}{E} \end{pmatrix}, & Q_{23} &= \begin{pmatrix} 0 & 0 \\ 0 & 0 \end{pmatrix}, \\
 Q_{24} &= \left(\frac{\gamma_3 SM}{E}, -\frac{\gamma_3 SM}{E} \right)^T, & Q_{31} &= \left(\frac{\gamma_2 E}{M}, 0 \right)^T, & Q_{32} &= \begin{pmatrix} \frac{\gamma_2 E}{M} & 0 \\ 0 & \frac{\gamma_2 E}{M} \end{pmatrix}, \\
 Q_{33} &= \begin{pmatrix} M_{33} - \frac{\dot{M}}{M} & -\beta_2 S - \mu_4 \\ q & M_{55} - \frac{\dot{M}}{M} \end{pmatrix}, & Q_{34} &= (-\beta_1 S - \mu_4, \beta_1 S - \mu_3)^T, & Q_{41} &= 0, \\
 Q_{42} &= (0, -\frac{\gamma_1 E}{M}), & Q_{43} &= (0, \mu_1), & Q_{44} &= M_{66} - \frac{\dot{M}}{M}.
 \end{aligned}$$

Hence, we have the following estimation (for an example, see [57–59]),

$$\sigma(Q(S, E, I, M)) \leq \sup\{g_1, g_2, g_3, g_4\},$$

where $g_1 = \sigma_1(Q_{11}) + |Q_{12}| + |Q_{13}| + |Q_{14}|$, $g_2 = \sigma_1(Q_{22}) + |Q_{21}| + |Q_{23}| + |Q_{24}|$, $g_3 = \sigma_1(Q_{33}) + |Q_{31}| + |Q_{32}| + |Q_{34}|$, $g_4 = \sigma_1(Q_{44}) + |Q_{41}| + |Q_{42}| + |Q_{43}|$. $|Q_{ij}|$ ($i \neq j, i, j = 1, 2, 3, 4$) are matrix norms with respect to the l_1 vector norm, and σ_1 denotes the Lozinski $\check{\sigma}$ measures with respect to the l_1 norm. Furthermore, it is easy to obtain that

$$\begin{aligned}
 \sigma(Q_{11}) &= -\beta_1 I - \beta_2 E - \gamma_3 M - 2d - \mu_4 + \beta_2 S - \mu_1 - \mu_3 - \frac{\dot{E}}{E}, \\
 \sigma(Q_{22}) &\leq -\mu_2 - 2d - \frac{\dot{E}}{E} + \max\{-\mu_4, 2\beta_2 S + \mu_4 - \mu_1 - \mu_3\}, \\
 \sigma(Q_{33}) &\leq -\rho - d - \frac{\dot{M}}{M} + \max\{-\mu_4, 2\beta_2 S + \mu_4 - \mu_1 - \mu_3\}, \\
 \sigma(Q_{44}) &= -d - \mu_2 - \rho - \frac{\dot{M}}{M}, & |Q_{12}| &= \beta_1 S + \mu_4, & |Q_{13}| &= \frac{\gamma_3 SM}{E}, \\
 |Q_{14}| &= 0, & |Q_{21}| &= \mu_1, & |Q_{23}| &= 0, & |Q_{24}| &= \frac{2\gamma_3 SM}{E}, & |Q_{31}| &= \frac{\gamma_2 E}{M}, \\
 |Q_{32}| &= \frac{\gamma_2 E}{M}, & |Q_{34}| &< 2\beta_1 S + \mu_4, & |Q_{41}| &= 0, & |Q_{42}| &= \frac{\gamma_1 E}{M}, & |Q_{43}| &= \mu_1.
 \end{aligned}$$

From condition (H2) and system (4), we have

$$\max\{-\mu_4, 2\beta_2 S + \mu_4 - \mu_1 - \mu_3\} = 2\beta_2 S + \mu_4 - \mu_1 - \mu_3,$$

and

$$\begin{aligned}
 \frac{\dot{E}}{E} &= \frac{\beta_1 SI}{E} + \beta_2 S + \frac{\gamma_3 SM}{E} + \frac{\mu_3 R}{E} - (d + \mu_1) > \frac{\beta_1 SI}{E} + \beta_2 S + \frac{\gamma_3 SM}{E} - (d + \mu_1), \\
 \frac{\dot{M}}{M} &= \frac{\gamma_1 E}{M} + \frac{\gamma_2 I}{M} - \rho > \frac{\gamma_1 E}{M} - \rho \geq \frac{\gamma_2 E}{M} - \rho.
 \end{aligned}$$

Hence, we have

$$\begin{aligned}
 g_1 &= -\beta_1 I - \beta_2 E - \gamma_3 M - 2d - \mu_4 + \beta_2 S - \mu_1 - \mu_3 - \frac{\dot{E}}{E} + \beta_1 S + \mu_4 + \frac{\gamma_3 SM}{E} \\
 &< -\beta_1 I - \beta_2 S - \gamma_3 M - \frac{\beta_1 SI}{E} - d - \mu_3 + \beta_1 S \\
 &< \frac{\beta_1 \Lambda}{d} - d - \mu_3 \equiv -\theta_1, \\
 g_2 &\leq -\mu_2 - 2d - \mu_3 - \frac{\dot{E}}{E} + 2\beta_2 S + \mu_4 - \mu_1 + \mu_1 + \frac{2\gamma_3 SM}{E} \\
 &< -\mu_2 - d - \mu_3 + \frac{\gamma_3 SM}{E} + \beta_2 S - \frac{\beta_1 SI}{E} + \mu_1 + \mu_4 \\
 &< \frac{\dot{E}}{E} + 2\mu_1 + \mu_4 - \mu_2 - \mu_3 \equiv \frac{\dot{E}}{E} - \theta_2, \\
 g_3 &< -\rho - \mu_3 - d - \frac{\dot{M}}{M} + 2\beta_2 S + \mu_4 - \mu_1 + \frac{2\gamma_2 E}{M} + 2\beta_1 S + \mu_4 \\
 &< \frac{\gamma_2 E}{M} - \rho + \rho - \mu_3 + (2\beta_1 + 2\beta_2)S + 2\mu_4 - d - \mu_1 \\
 &< \frac{\dot{M}}{M} + (2\beta_1 + 2\beta_2) \frac{\Lambda}{d} + \rho + 2\mu_4 - d - \mu_1 - \mu_3 \equiv \frac{\dot{M}}{M} - \theta_3, \\
 g_4 &= -d - \mu_2 - \rho - \frac{\dot{M}}{M} + \frac{\gamma_1 E}{M} + \mu_1 \\
 &< \mu_1 - d - \mu_2 \equiv -\theta_4.
 \end{aligned}$$

Again, from condition (H2), we can obtain

$$\theta_3 < \theta_1, \quad \bar{b} = \min\{\theta_1, \theta_2, \theta_3, \theta_4\} = \min\{\theta_2, \theta_3, \theta_4\} > 0,$$

and

$$g_1 \leq -\bar{b}, \quad g_2 < \frac{\dot{E}}{E} - \bar{b}, \quad g_3 < \frac{\dot{M}}{M} - \bar{b}, \quad g_4 \leq -\bar{b}.$$

Note that when $\mathcal{R}_0 > 1$, system (4) is uniformly persistent. Using a similar argument as in [59], we find that the endemic equilibrium Q^* of system (4) is globally asymptotically stable. \square

Take $\Lambda = 1000$, $\beta_1 = 5 \times 10^{-7}$, $\beta_2 = 5 \times 10^{-7}$, $\gamma_1 = 2 \times 10^{-3}$, $\gamma_2 = 2 \times 10^{-3}$, $\gamma_3 = 2 \times 10^{-3}$, $\mu_1 = 0.2$, $\mu_2 = 0.5$, $\mu_3 = 0.1$, $\mu_4 = 0.15$, $d = 0.1$, $d_1 = 0.1$, $d_2 = 0.1$, and $\rho = 0.05$. Using numerical calculations, we obtain the basic reproduction number $R_0 = 2.625 > 1$, and the inequalities in (H1)–(H2) hold.

3. Applications of the Model in Japan and Italy

In this section, we use model (1) to fit the data of confirmed cases and recovered cases of COVID-19 in Japan and Italy (data were taken from the Johns Hopkins University Center for Systems Science and Engineering, <https://github.com/CSSEGISandData/COVID-19> accessed on 1 July 2022), and make short-term predictions about disease infection trends. Meanwhile, based on the basic reproduction number R_0 and data in Italy, we carried out a sensitivity analysis and the main factors related to disease transmission were captured.

3.1. Predicted Cases for Cumulative Confirmed and Recovered Cases Based on Data in Japan and Italy

First, from [3,60–62] and data published by the World Health Organization (WHO), the parameters $\frac{1}{\mu_1}$ (incubation period), $\frac{1}{\mu_2}$ (infectious period), $\frac{1}{\mu_4}$ (time of immune protection), $\frac{1}{d}$ (mean lifetime), and d_2 (death rate of the infected individuals caused by the virus) in model (1) can take the values as shown in Table 2 below. Furthermore, by using data of COVID-19 in Japan (20 May–18 June 2022) and Italy (12 January–10 February 2022) and the

least squares method (LSM), the remaining parameters in model (1) take values as shown in Table 2 below.

Table 2. The estimated values of parameters in the model.

| Para-Meter | Definitions | Value (Japan) | Value (Italy) | Unit | Source |
|---------------------|---------------------------|------------------------|------------------------|--|--------|
| β_1 | See Table 1 | 2.744×10^{-7} | 3.195×10^{-6} | /10,000 persons \times day | LSM |
| β_2 | See Table 1 | 6.766×10^{-7} | 5.123×10^{-6} | /10,000 persons \times day | LSM |
| γ_1 | See Table 1 | 0.6513 | 0.3966 | 10,000 viruses/10,000 persons \times day | LSM |
| γ_2 | See Table 1 | 0.2791 | 0.6091 | 10,000 viruses/10,000 persons \times day | LSM |
| γ_3 | See Table 1 | 1.559×10^{-8} | 5.235×10^{-7} | /10,000 viruses \times day | LSM |
| ρ | See Table 1 | 0.8901 | 0.5957 | /day | LSM |
| Λ | See Table 1 | 0.3916 | 0.3358 | 10,000 persons/day | LSM |
| $\frac{1}{\mu_1}$ | Incubation period | 5.2 | 5.2 | day | [3] |
| $\frac{1}{\mu_2}$ | Infectious period | 20 | 20 | day | [60] |
| μ_3 | See Table 1 | 0.03051 | 0.09186 | /day | LSM |
| $\frac{1}{\mu_4}$ | Time of immune protection | 180 | 180 | day | [61] |
| $\frac{1}{\bar{d}}$ | Mean lifetime | 84×365 | 83×365 | day | WHO |
| d_1 | See Table 1 | 2.025×10^{-4} | 3.371×10^{-4} | /day | LSM |
| d_2 | See Table 1 | 1.425×10^{-3} | 2.512×10^{-3} | /day | [62] |

Based on the parameter values given in Table 2, we obtain Figure 2a,b, which shows that model (1) fits well with the evolution of cumulative confirmed cases and recovered cases in Japan from 20 May–18 June 2022. Similarly, we have Figure 3a,b that shows that model (1) also fits well with the evolution of the cumulative confirmed cases and recovered cases in Italy from 12 January–10 February 2022.

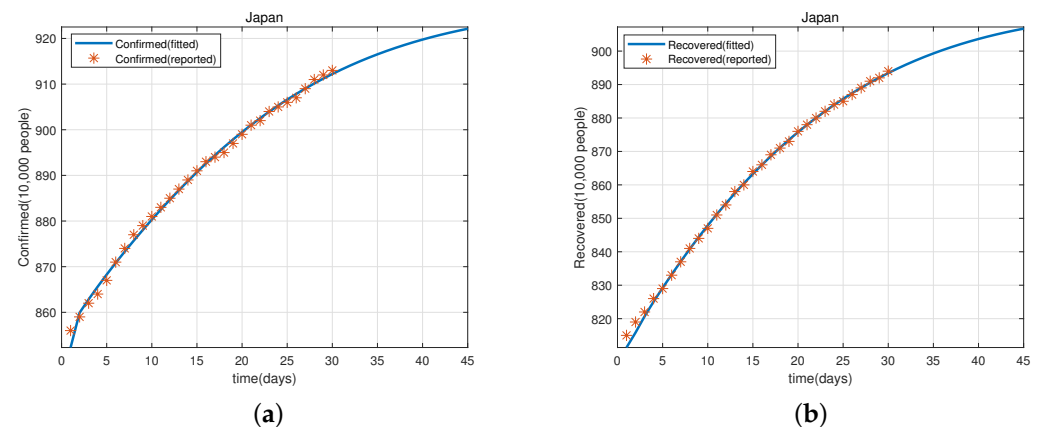


Figure 2. (a) The evolution of the cumulative confirmed cases of COVID-19 in Japan from 20 May–18 June 2022. (b) The evolution of the cumulative recovered cases of COVID-19 in Japan from 20 May–18 June 2022.

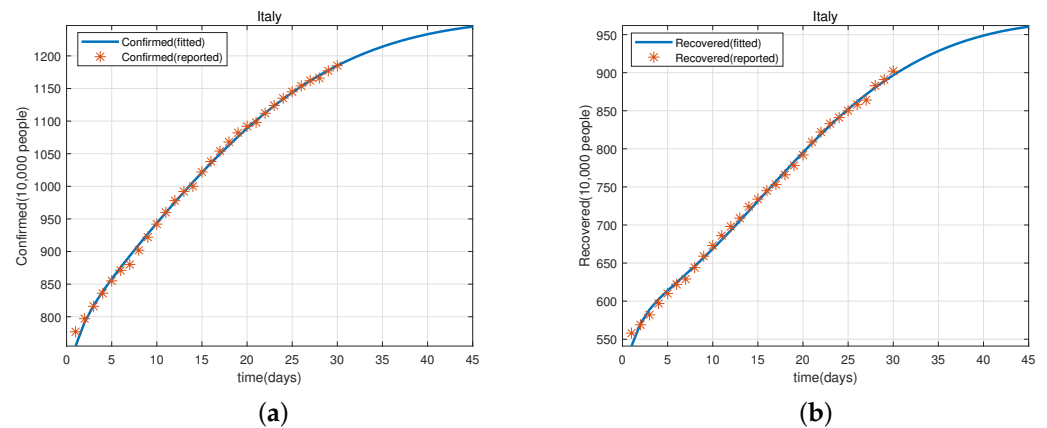


Figure 3. (a) The evolution of the cumulative confirmed cases of COVID-19 in Italy from 12 January–10 February 2022. (b) The evolution of the cumulative recovered cases of COVID-19 in Italy from 12 January–10 February 2022.

Next, we use model (1) and the parameter values given in Table 2 to predict the cumulative confirmed cases and recovered cases in Japan (from 19–28 June 2022) and Italy (from 11–20 February 2022). These are shown in Tables 3–6.

From Tables 3–6, it can be seen that the predicted values for confirmed and recovered cases are within a range of 97 to 103% of the reported data. With the increase in time t , the relative error also increases.

Table 3. Predicted values and reported data for confirmed cases in Japan.

| Data | Cumulative Confirmed Cases (Japan) | |
|------|------------------------------------|-----------|
| | Reported | Predicted |
| 6.19 | 917.2745 | 912.8151 |
| 6.20 | 920.0541 | 913.6510 |
| 6.21 | 923.5918 | 914.4373 |
| 6.22 | 927.3191 | 915.1782 |
| 6.23 | 930.9861 | 915.8729 |
| 6.24 | 931.5674 | 916.5263 |
| 6.25 | 933.2259 | 917.1391 |
| 6.26 | 934.6495 | 917.7133 |
| 6.27 | 935.6060 | 918.2511 |
| 6.28 | 936.5433 | 918.7538 |

Table 4. Predicted values and reported data for recovered cases in Japan.

| Data | Cumulative Recovered Cases (Japan) | |
|------|------------------------------------|-----------|
| | Reported | Predicted |
| 6.19 | 897.7861 | 894.7521 |
| 6.20 | 900.3232 | 895.9912 |
| 6.21 | 903.6874 | 897.1613 |
| 6.22 | 905.2890 | 898.2644 |
| 6.23 | 908.7801 | 899.3047 |
| 6.24 | 910.2259 | 900.2809 |
| 6.25 | 914.0274 | 901.1989 |
| 6.26 | 916.9366 | 902.0616 |
| 6.27 | 917.9099 | 902.8693 |
| 6.28 | 918.6873 | 903.0266 |

Table 5. Predicted values and reported data for confirmed cases in Italy.

| Data | Cumulative Confirmed Cases (Italy) | |
|------|------------------------------------|-----------|
| | Reported | Predicted |
| 2.11 | 1201.3631 | 1191.4833 |
| 2.12 | 1212.1109 | 1198.4161 |
| 2.13 | 1220.3330 | 1203.0440 |
| 2.14 | 1228.5675 | 1209.3611 |
| 2.15 | 1236.4451 | 1214.3588 |
| 2.16 | 1242.5474 | 1218.0709 |
| 2.17 | 1250.5343 | 1223.4792 |
| 2.18 | 1255.3398 | 1226.6014 |
| 2.19 | 1260.7098 | 1230.4304 |
| 2.20 | 1266.1773 | 1233.9731 |

Table 6. Predicted values and reported data for recovered cases in Italy.

| Data | Cumulative Recovered Cases (Italy) | |
|------|------------------------------------|-----------|
| | Reported | Predicted |
| 2.11 | 908.0136 | 904.2121 |
| 2.12 | 918.9429 | 911.0671 |
| 2.13 | 927.6892 | 917.8210 |
| 2.14 | 934.5987 | 923.4734 |
| 2.15 | 940.2540 | 928.2089 |
| 2.16 | 946.3380 | 933.3926 |
| 2.17 | 953.3268 | 938.6280 |
| 2.18 | 960.2908 | 942.6809 |
| 2.19 | 966.0380 | 946.5611 |
| 2.20 | 970.5147 | 949.2560 |

Furthermore, we use MAPE (mean absolute percentage error) and RMSPE (root mean square error) to assess the reliability of model (1) in data fitting (for examples, see [63,64]). For convenience, we introduce the definitions of MAPE and RMSPE and their evaluation standard, as follows (Table 7):

$$MAPE = \frac{\sum_{i=1}^n \left| \frac{y_i - y'_i}{y_i} \right|}{n} \times 100\%, \quad RMSPE = \sqrt{\frac{\sum_{i=1}^n \left[\frac{y_i - y'_i}{y_i} \right]^2}{n - 1}} \times 100\%$$

Table 7. MAPE/RMSPE evaluation standard.

| MAPE/RMSPE | Predictive Ability |
|------------|-------------------------|
| <10% | Precision prediction |
| 10–20% | Good prediction |
| 20–50% | Reasonable prediction |
| >50% | Unreasonable prediction |

Here, y_i and y'_i are the reported data and predicted data, respectively, and the positive integer n is the number of predicted data. Using the data in Tables 3–6, we obtain Table 8.

Table 8. MAPE/RMSPE values and their predictive ability.

| Data Type | MAPE | Predictive Ability | RMSPE | Predictive Ability |
|--------------------------|-------|----------------------|-------|----------------------|
| Confirmed cases in Japan | 1.40% | Precision prediction | 1.56% | Precision prediction |
| Reovered cases in Japan | 1.08% | Precision prediction | 1.24% | Precision prediction |
| Confirmed cases in Italy | 1.81% | Precision prediction | 1.99% | Precision prediction |
| Recovered cases in Italy | 1.38% | Precision prediction | 1.55% | Precision prediction |

3.2. Sensitivity Analysis Based on the Basic Reproduction Number and Data from Italy

From Theorem 1 and 2 we see that if the basic reproduction number $\mathcal{R}_0 < 1$ (or $\mathcal{R}_0 > 1$), the disease infection can be cleared (or will become an endemic disease). Therefore, it is very necessary to make a sensitivity analysis based on the basic reproduction number \mathcal{R}_0 , and then capture the main factors related to disease transmission.

The normalized sensitivity index of \mathcal{R}_0 is defined as $\gamma_\epsilon^{\mathcal{R}_0} \equiv \frac{\partial \mathcal{R}_0}{\partial \epsilon} \frac{\epsilon}{\mathcal{R}_0}$. Here, ϵ can be regarded as any parameter in \mathcal{R}_0 [65]. By using Italy's parameter values in Table 3, we obtain Table 9 and Figure 4.

Table 9. The normalized sensitivity index based on \mathcal{R}_0 and data from Italy.

| | | | | | | |
|-----------------------------|------------|------------|------------|---------|---------|---------|
| Parameter Sensitivity Index | β_1 | β_2 | μ_1 | μ_2 | μ_3 | μ_4 |
| | 0.5827 | 0.2993 | −0.2501 | −0.1816 | 0.2618 | −0.0833 |
| Parameter Sensitivity Index | γ_1 | γ_2 | γ_3 | ρ | d_1 | d_2 |
| | 0.0200 | 0.0979 | 0.1180 | −0.1180 | −0.0041 | −0.0713 |

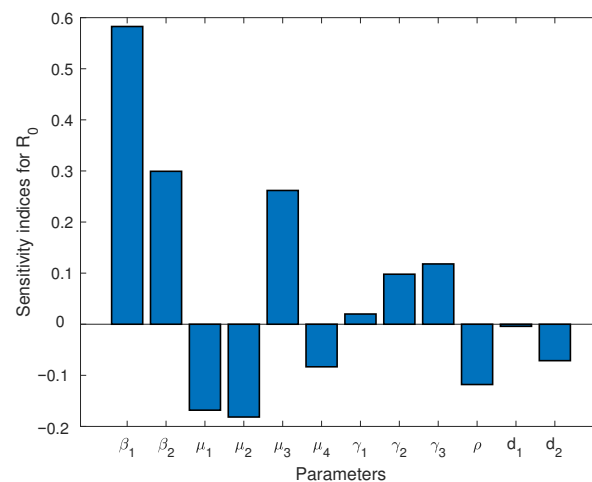


Figure 4. The normalized sensitivity index based on \mathcal{R}_0 and data from Italy.

From Table 9 and Figure 4, we first observe that the parameters β_1 (the infection rate of infected individuals) and β_2 (the infection rate of exposed individuals) are the most sensitive (and positively correlated) parameters to the basic reproduction number \mathcal{R}_0 . When β_1 increases by 10% while other parameters remain unchanged, R_0 increases by 5.827%. Similarly, when β_2 increases by 10% while other parameters remain unchanged, R_0 increases by 2.993%. Moreover, the parameters μ_1 (the rate at which exposed individuals become infected) and μ_2 (the recovery rate of infected people) also have high sensitivities (but are negatively correlated) to the basic reproduction number \mathcal{R}_0 . When μ_1 increases by 10% while other parameters remain unchanged, R_0 decreases by 2.501%. Similarly, when μ_2 increases by 10% while other parameters remain unchanged, R_0 decreases by 1.816%.

On the other hand, we also see from Table 9 and Figure 4 that the basic reproduction number \mathcal{R}_0 has a strong dependence (positively/negatively correlated) on environmental and re-positive factors. Specifically, the parameters μ_3 (the rate of re-positives), γ_2 (the rate of virus release into the environment by infected individuals), γ_3 (the infection rate due to environmental vectors), and ρ (the rate at which the free virus particles decay or are cleared in environmental vectors) are also more sensitive to the basic reproduction number \mathcal{R}_0 . When γ_2 , γ_3 , and μ_3 increases by 10% while other parameters remain unchanged, R_0 increases by 0.979, 1.180 and 2.618%, respectively; however, when ρ increases by 10%, R_0 decreases by 1.180%.

This suggests that we should strengthen prevention and control to reduce the transmission rate of the disease, shorten the treatment cycle, increase antibodies by vaccination, pay attention to environmental sanitation, and reduce the risk of environmental infection.

At the end of this subsection, we present a discussion of the control strategies related to environmental and re-positive factors using the basic reproduction number \mathcal{R}_0 .

Consider the basic reproduction number \mathcal{R}_0 as a function $\mathcal{R}_0 = \mathcal{R}_0(\mu_3, \gamma_3)$ with respect to the parameters μ_3 and γ_3 , and let the values of all the other parameters in the basic reproduction number \mathcal{R}_0 be the same as those from Italy in Table 3.

Figure 5a gives the intersection line of the surface $\mathcal{R}_0 = \mathcal{R}_0(\mu_3, \gamma_3)$ and the plane $\mathcal{R}_0 = 1$. Figure 5b shows the contour lines corresponding to the different values of \mathcal{R}_0 . The contour lines give the range of the parameters, μ_3 and γ_3 , which are directly related to environmental and re-positive factors. Particularly, the area on the right side of the contour line with $\mathcal{R}_0 = 1$ can be seen as a high-risk area, which means that the disease infection will exist forever, and the area on the left side of the contour line with $\mathcal{R}_0 = 1$ can be seen as a low-risk area, which means that the disease infection will eventually be cleared. That is, when the parameter related to environmental factors (γ_3) and the parameter related to re-positives (μ_3) have their values in the low-risk area, the disease infection is controllable.

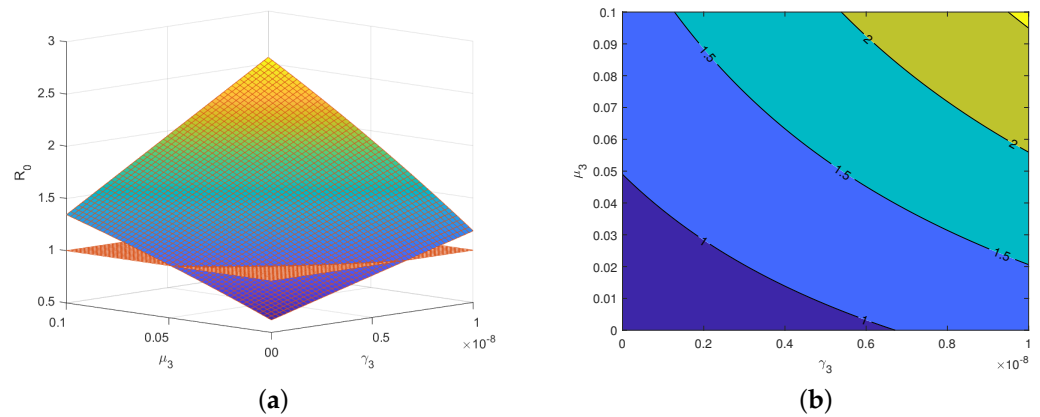


Figure 5. (a) The intersection line of $\mathcal{R}_0 = \mathcal{R}_0(\mu_3, \gamma_3)$ and $\mathcal{R}_0 = 1$. (b) Contour lines corresponding to different values of \mathcal{R}_0 .

Moreover, Figure 6a,b shows that when the parameters γ_3 (the infection rate due to environmental vectors) or μ_3 (the rate of re-positives) decreases, the cumulative number of infected cases also decreases significantly.

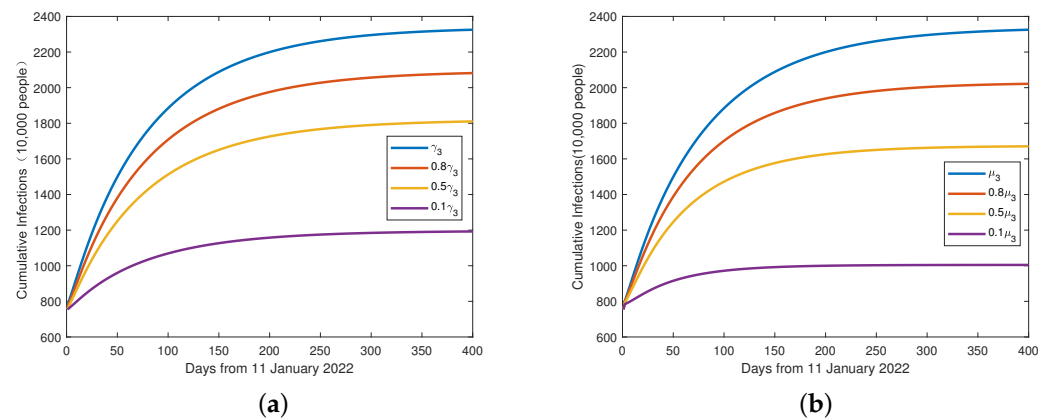


Figure 6. (a) The evolutionary relationship between the cumulative number of infected cases (I) and the parameter γ_3 . (b) The evolutionary relationship between the cumulative number of infected cases (I) and the parameter μ_3 .

According to the above figures, the re-positive rate μ_3 decreased 10 times, and the cumulative number of infected cases decreased 48%. This is alarming, and suggests we need to pay more attention to recovered patients and their potential infectivity. We may need to re-evaluate hospitals' discharge criteria and current patient management systems. Therefore, we stress that caution should be exercised even after recovery from SARS-CoV-2. We believe that all discharged patients should undergo medical observation and quarantine for at least 14 days. Longer periods of observation and surveillance may be necessary. Patients who have been infected with COVID-19 virus in the past should also comply with epidemiological control measures, such as wearing a mask and keeping distance from others.

The environment-related parameter γ_3 decreased 10 times, and the cumulative number of infected cases decreased 58%. However, some recent research has shown that there are many ways of communication for the novel coronavirus, and communication by environmental vectors is an important link that cannot be ignored. When an infected person sneezes or coughs, droplets are released that can contaminate surfaces. If a susceptible person touches these contaminated surfaces and then touches their mouth, nose, or eyes, they can become infected. If we want to ensure that the virus does not spread on a large scale, it is very important to sanitize the environment. For normal households, sanitizing with alcohol and disinfectant water can meet the demand, and families with susceptible conditions can also purchase ozone disinfection equipment for sanitizing. For places with local epidemic break-out, professional institutions are needed for sanitization. We have obtained some crucial epidemiological parameters that need greater emphasis for the mitigation and control of the COVID-19 pandemic.

4. Conclusions

Inspired by the diversity and complexity of COVID-19 infections, two key factors were considered in model (1). The first is that environmental vectors polluted by virus particles may lead to disease infection, and the second is that recovered individuals who have lost sufficient immune protection may return to the exposed class (i.e., called re-positive). In the past two years especially, these factors have been increasingly observed in the spread of COVID-19 infection, and are bringing great challenges and difficulties to the control of disease infection.

Theorems 1 and 2 give a complete characterization of the global dynamics of model (1). In other words, when the basic reproduction number $\mathcal{R}_0 < 1$, the disease-free equilibrium Q_0 is globally asymptotically stable, meaning that the disease infection will eventually be cleared. When the basic reproduction number $\mathcal{R}_0 > 1$, model (1) is uniformly persistent, meaning that the disease infection will exist forever and become an endemic disease. Furthermore, Theorem 3 gives some sufficient conditions for the global asymptotic stability of the endemic equilibrium Q^* of model (1). It should be mentioned here that the sufficient conditions in Theorem 3 are very conservative and can be further improved.

Model (1) was applied to the data fitting of the cumulative confirmed cases and recovered cases of COVID-19 in Japan (20 May–18 June 2022) and Italy (12 January–10 February 2022), and good predictability of the data was observed.

Furthermore, based on data from Italy (12 January–10 February 2022), it was observed that the basic reproduction number \mathcal{R}_0 also had stronger dependence on the parameters μ_3 , γ_2 , γ_3 , and ρ . This indicates the necessity and practical significance of considering environmental and re-positive factors in the prevention and control of COVID-19 infection.

Author Contributions: Conceptualization, S.D. and W.M.; methodology, S.D.; software, J.L. and S.D.; writing—original draft preparation, S.D.; writing—review and editing, W.M. and B.G.S.A.P. All authors have read and agreed to the published version of the manuscript.

Funding: This paper is supported by the National Natural Science Foundation of China (No. 11971055) and the Beijing Natural Science Foundation, China (No. 1202019).

Institutional Review Board Statement: Not applicable.

Informed Consent Statement: Not applicable.

Data Availability Statement: The data used for the numerical simulation analysis are from the Johns Hopkins University Center for Systems Science and Engineering, <https://github.com/CSSEG/ISandData/COVID-19> (accessed on 1 July 2022).

Conflicts of Interest: The authors declare no conflict of interest.

References

1. Coronaviridae Study Group of the International Committee on Taxonomy of Viruses. The species Severe acute respiratory syndrome-related coronavirus: Classifying 2019-nCoV and naming it SARS-CoV-2. *Nat. Microbiol.* **2020**, *5*, 536–544. [[CrossRef](#)] [[PubMed](#)]
2. Zhou, P.; Yang, X.L.; Wang, X.G.; Hu, B.; Zhang, L.; Zhang, W.; Si, H.R.; Zhu, Y.; Li, B.; Huang, C.L.; et al. A pneumonia outbreak associated with a new coronavirus of probable bat origin. *Nature* **2020**, *579*, 270–273. [[CrossRef](#)] [[PubMed](#)]
3. Li, Q.; Guan, X.H.; Wu, P.; Wang, X.; Zhou, L.; Tong, Y.; Ren, R.; Leung, K.S.; Lau, E.H.; Wong, J.Y.; et al. Early Transmission Dynamics in Wuhan, China, of Novel Coronavirus-Infected Pneumonia. *N. Engl. J. Med.* **2020**, *382*, 1199–1207. [[CrossRef](#)] [[PubMed](#)]
4. Coronavirus-Public Health Emergency. Available online: <https://time.com/5774747/coronavirus-whopublic-health-emergency/> (accessed on 11 July 2020).
5. COVID-19 Biggest Global Crisis for Children in Our 75-Year History. Available online: <https://www.unicef.cn/press-releases/covid-19-biggest-global-crisis-children-our-75-year-history-unicef> (accessed on 18 July 2021).
6. Dennis, A.; Wamil, M.; Alberts, J.; Oben, J.; Cuthbertson, D.J.; Wootton, D.; Crooks, M.; Gabbay, M.; Brady, M.; Hishmeh, L.; et al. Multiorgan impairment in low-risk individuals with post-COVID-19 syndrome: A prospective, community-based study. *BMJ Open* **2021**, *11*, e048391. [[CrossRef](#)] [[PubMed](#)]
7. Huang, C.L.; Huang, L.X.; Wang, Y.M.; Li, X.; Ren, L.; Gu, X.; Kang, L.; Guo, L.; Liu, M.; Zhou, X.; et al. 6-month consequences of covid-19 in patients discharged from hospital: A cohort study. *Lancet* **2021**, *397*, 220–232. [[CrossRef](#)] [[PubMed](#)]
8. WHO Coronavirus (COVID-19) Dashboard. Available online: <https://covid19.who.int> (accessed on 22 August 2022).
9. Coronavirus Disease 2019 (COVID-19) Treatment Guidelines. Available online: <https://www.covid19treatmentguidelines.nih.gov/> (accessed on 18 July 2022).
10. Dagan, N.; Barda, N.; Kepten, E.; Miron, O.; Perchik, S.; Katz, M.A.; Hernán, M.A.; Lipsitch, M.; Reis, B.; Balicer, R.D. BNT162b2 mRNA Covid-19 Vaccine in a Nationwide Mass Vaccination Setting. *N. Engl. J. Med.* **2021**, *384*, 1412–1423. [[CrossRef](#)] [[PubMed](#)]
11. Tang, B.; Xia, F.; Wu, J.H. Lessons drawn from China and South Korea for managing COVID-19 epidemic: Insights from a comparative modeling study. *ISA Trans.* **2020**, *124*, 164–175. [[CrossRef](#)] [[PubMed](#)]
12. Tang, B.; Wang, X.; Li, Q.; Bragazzi, N.L.; Tang, S.; Xiao, Y.; Wu, J. Estimation of the Transmission Risk of the 2019-nCoV and Its Implication for Public Health Interventions. *J. Clin. Med.* **2020**, *9*, 462. [[CrossRef](#)]
13. Yang, Z.F.; Zeng, Z.Q.; Wang, K.; Wong, S.S.; Liang, W.; Zanin, M.; Liu, P.; Cao, X.; Gao, Z.; Mai, Z.; et al. Modified SEIR and AI prediction of the epidemics trend of COVID-19 in China under public health interventions. *J. Thorac. Dis.* **2020**, *12*, 165–174. [[CrossRef](#)]
14. Kucharski, A.J.; Russell, T.W.; Diamond, C.; Liu, Y.; Edmunds, J.; Funk, S.; Eggo, R.M.; Sun, F.; Jit, M.; Munday, J.D.; et al. Early dynamics of transmission and control of COVID-19: A mathematical modelling study. *Lancet Infect. Dis.* **2020**, *20*, 553–558. [[CrossRef](#)]
15. Sarkar, K.; Khajanchi, S.; Nieto, J.J. Modeling and forecasting the COVID-19 pandemic in India. *Chaos Solitons Fractals* **2020**, *139*, 110049. [[CrossRef](#)] [[PubMed](#)]
16. Nadim, S.S.; Chattopadhyay, J. Occurrence of backward bifurcation and prediction of disease transmission with imperfect lockdown: A case study on COVID-19. *Chaos Solitons Fractals* **2020**, *140*, 110163. [[CrossRef](#)] [[PubMed](#)]
17. Yang, C.Y.; Wang, J. A mathematical model for the novel coronavirus epidemic in Wuhan, China. *Math. Biosci. Eng.* **2020**, *17*, 2708–2724. [[CrossRef](#)] [[PubMed](#)]
18. Rong, X.M.; Yang, L.; Chu, H.D.; Fan, M. Effect of delay in diagnosis on transmission of COVID-19. *Math. Biosci. Eng.* **2020**, *17*, 2725–2740. [[CrossRef](#)]
19. Anastassopoulou, C.; Russo, L.; Tsakris, A.; Siettos, C. Data-based analysis, modelling and forecasting of the COVID-19 outbreak. *PLoS ONE* **2020**, *15*, e0230405. [[CrossRef](#)]
20. Zhang, T.L.; Li, Z.M. Analysis of COVID-19 epidemic transmission trend based on a time-delayed dynamic model. *Commun. Pure Appl. Anal.* **2023**, *22*, 1–18. [[CrossRef](#)]
21. Li, T.J.; Xiao, Y.N. Linking the disease transmission to information dissemination dynamics: An insight from a multi-scale model study. *J. Theor. Biol.* **2021**, *526*, 110796. [[CrossRef](#)]
22. Zu, J.; Shen, M.W.; Li, Y. Investigating the relationship between reopening the economy and implementing control measures during the COVID-19 pandemic. *Public Health* **2021**, *200*, 15e21. [[CrossRef](#)]
23. Duan, M.; Jin, Z. The heterogeneous mixing model of COVID-19 with interventions. *J. Theor. Biol.* **2022**, *553*, 111258. [[CrossRef](#)]
24. Tu, H.; Wang, X.; Tang, S. Exploring COVID-19 transmission patterns and key factors during epidemics caused by three major strains in Asia. *J. Theor. Biol.* **2023**, *557*, 111336. [[CrossRef](#)]

25. Zhou, W.; Tang, B.; Tang, S. The resurgence risk of COVID-19 in China in the presence of immunity waning and ADE: A mathematical modelling study. *Vaccine* **2022**, *40*, 7141–7150. [[CrossRef](#)] [[PubMed](#)]
26. Yuan, B.; Liu, R.; Tang, S. A quantitative method to project the probability of the end of an epidemic: Application to the COVID-19 outbreak in Wuhan. *J. Theor. Biol.* **2022**, *545*, 111149. [[CrossRef](#)] [[PubMed](#)]
27. Pang, D.F.; Xiao, Y.N.; Zhao, X.Q. A cross-infection model with diffusive environmental bacteria. *J. Math. Anal. Appl.* **2022**, *505*, 125637. [[CrossRef](#)]
28. Kampf, G.; Todt, D.; Pfaender, S.; Steinmann, E. Persistence of coronaviruses on inanimate surfaces and their inactivation with biocidal agents. *J. Hosp. Infect.* **2020**, *104*, 246–251. [[CrossRef](#)] [[PubMed](#)]
29. Doremalen, N.V.; Bushmaker, T.; Morris, D.H.; Holbrook, M.G.; Gamble, A.; Williamson, B.N.; Tamin, A.; Harcourt, J.L.; Thornburg, N.J.; Gerber, S.I.; et al. Aerosol and Surface Stability of SARS-CoV-2 as Compared with SARS-CoV-1. *N. Engl. J. Med.* **2020**, *382*, 1564–1567. [[CrossRef](#)] [[PubMed](#)]
30. Nourbakhsh, S.; Fazil, A.; Li, M.; Mangat, C.S.; Peterson, S.W.; Daigle, J.; Langner, S.; Shurgold, J.; D’Aoust, P.; Delatolla, R.; et al. A wastewater-based epidemic model for SARS-CoV-2 with application to three Canadian cities. *Epidemics* **2022**, *39*, 100560. [[CrossRef](#)]
31. Vallejo, J.A.; Trigo-Tasende, N.; Rumbo-Feal, S.; Conde-Pérez, K.; López-Oriona, Á.; Barbeito, I.; Vaamonde, M.; Tarrío-Saavedra, J.; Reif, R.; Ladra, S.; et al. Modeling the number of people infected with SARS-COV-2 from wastewater viral load in Northwest Spain. *Sci. Total Environ.* **2021**, *811*, 152334–152334. [[CrossRef](#)]
32. Bai, J.; Wang, J. A two-patch model for the COVID-19 transmission dynamics in China. *J. Appl. Anal. Comput.* **2021**, *11*, 1982–2016. [[CrossRef](#)]
33. Naik, P.A.; Zu, J.; Ghori, M.B.; Naik, M. Modeling the effects of the contaminated environments on COVID-19 transmission in India. *Results Phys.* **2021**, *29*, 104774. [[CrossRef](#)]
34. Rai, R.K.; Khajanchi, S.; Tiwari, P.K.; Venturino, E.; Misra, A.K. Impact of social media advertisements on the transmission dynamics of COVID-19 pandemic in India. *J. Appl. Math. Comput.* **2022**, *68*, 19–44. [[CrossRef](#)]
35. Chen, T.M.; Rui, J.; Wang, Q.X.; Zhao, Z.Y.; Cui, J.A.; Yin, L. A mathematical model for simulating the phase-based transmissibility of a novel coronavirus. *Infect. Dis. Poverty.* **2020**, *9*, 24. [[CrossRef](#)] [[PubMed](#)]
36. Xiao, Y.N.; Tang, S.Y.; Wu, J.H. Media impact switching surface during an infectious disease outbreak. *Sci. Rep.* **2015**, *5*, 7838. [[CrossRef](#)] [[PubMed](#)]
37. Huo, H.F.; Yang, P.; Xiang, H. Stability and bifurcation for an SEIS epidemic model with the impact of media. *Phys. A* **2018**, *490*, 702–720. [[CrossRef](#)]
38. Cui, J.A.; Sun, Y.H.; Zhu, H.P. The impact of media on the control of infectious diseases. *J. Dyn. Differ. Equ.* **2008**, *20*, 31–53. [[CrossRef](#)]
39. Yan, Q.L.; Tang, S.Y.; Gabriele, S.; Wu, J.H. Media coverage and hospital notifications: Correlation analysis and optimal media impact duration to manage a pandemic. *J. Theor. Biol.* **2016**, *390*, 1–13. [[CrossRef](#)] [[PubMed](#)]
40. Song, P.F.; Xiao, Y.N. Analysis of an Epidemic System with Two Response Delays in Media Impact Function. *Bull. Math. Biol.* **2019**, *81*, 1582–1612. [[CrossRef](#)]
41. Musa, S.S.; Yusuf, A.; Zhao S.; Abdullahi, Z.U.; Abu-Odah, H.; Saad, F.T.; Adamu, L.; He, D. Transmission dynamics of COVID-19 pandemic with combined effects of relapse, reinfection and environmental contribution: A modeling analysis. *Results Phys.* **2022**, *38*, 105653. [[CrossRef](#)]
42. Garba, S.M.; Lubuma, J.M.; Tsanou, B. Modeling the transmission dynamics of the COVID-19 pandemic in South Africa. *Math Biosci.* **2020**, *328*, 108441. [[CrossRef](#)]
43. Lan, L.; Xu, D.; Ye, G.; Xia, C.; Wang, S.; Li, Y.; Xu, H. Positive RT-PCR test results in patients recovered from COVID-19. *JAMA* **2020**, *323*, 1502–1503. [[CrossRef](#)]
44. Mei, Q.; Li, J.; Du, R.; Yuan, X.; Li, M.; Li, J. Assessment of patients who tested positive for COVID-19 after recovery. *Lancet Infect. Dis.* **2020**, *20*, 1004–1005. [[CrossRef](#)]
45. Tang, X.; Zhao, S.; He, D.; Yang, L.; Wang, M.H.; Li, Y.; Mei, S.; Zou, X. Positive RT-PCR tests among discharged COVID-19 patients in Shenzhen, China. *Infect Control. Hosp Epidemiol.* **2020**, *41*, 1110–1112. [[CrossRef](#)] [[PubMed](#)]
46. An, J.; Liao, X.; Xiao, T.; Qian, S.; Yuan, J.; Ye, H.; Qi, F.; Shen, C.; Wang, L.; Liu, Y.; et al. Clinical characteristics of recovered COVID-19 patients with re-detectable positive RNA test. *Ann. Transl. Med.* **2020**, *8*, 1084. [[CrossRef](#)] [[PubMed](#)]
47. To, K.K.; Hung, I.F.; Chu, A.W.; Chan, W.M.; Chan, W.M.; Tam, A.R.; Fong, C.H.; Yuan, S.; Tsoi, H.W.; Ng, A.C.; et al. COVID-19 re-infection by a phylogenetically distinct SARS-coronavirus-2 strain confirmed by whole genome sequencing. *Clin. Infect. Dis.* **2020**, ciaa1275. [[CrossRef](#)]
48. Murillo-Zamora, E.; Mendoza-Cano, O.; Delgado-Enciso, I.; Hernandez-Suarez, C.M. Predictors of severe symptomatic laboratory-confirmed SARS-COV-2 reinfection. *Public Health* **2021**, *193*, 113–115. [[CrossRef](#)]
49. Buskermolen, M.; Paske, K.; Beek, J.; Kortbeek, T.; Götz, H.; Fanoy, E.; Feenstra, S.; Richardus, J.H.; Vollaard, A. Relapse in the first 8 weeks after onset of COVID-19 disease in outpatients: Viral reactivation or inflammatory rebound? *J. Infect.* **2021**, *83*, e6–e8. [[CrossRef](#)] [[PubMed](#)]
50. Reinfection with SARS-CoV: Considerations for Public Health Response: ECDC. Available online: <https://www.ecdc.europa.eu/> (accessed on 18 August 2021).

51. Diekmann, O.; Heesterbeek, J.A.P.; Metz, J.A.J. On the definition and the computation of the basic reproduction ratio R_0 in models for infectious diseases in heterogeneous populations. *J. Math. Biol.* **1990**, *28*, 365–382. [[CrossRef](#)] [[PubMed](#)]
52. Driessche, P.V.D.; Watmough, J. Reproduction numbers and sub-threshold endemic equilibria for compartmental models of disease transmission. *Math. Biosci.* **2002**, *180*, 29–48. [[CrossRef](#)]
53. Wang, W.D. Global behavior of an SEIRS epidemic model with time delays. *Appl. Math. Lett.* **2002**, *15*, 423–428. [[CrossRef](#)]
54. Guo, S.B.; Ma, W.B. Global behavior of delay differential equations model of HIV infection with apoptosis. *Discret. Contin. Dyn. Syst.-Ser. B* **2015**, *21*, 103–119. [[CrossRef](#)]
55. Guo, S.; Jiang, W.H.; Wang, H.B. Global analysis in delayed ratio-dependent gause-type predator-prey models. *J. Appl. Anal. Comput.* **2017**, *7*, 1095–1111. [[CrossRef](#)]
56. Guo, K.; Ma, W.B. Permanence and extinction for a nonautonomous Kawasaki disease model with time delays. *Appl. Math. Lett.* **2021**, *122*, 107511. [[CrossRef](#)]
57. Martin, R.H. Logarithmic norms and projections applied to linear differential systems. *J. Math. Anal. Appl.* **1974**, *45*, 432–454. [[CrossRef](#)]
58. Li, M.Y.; Muldowney, J.S. A Geometric Approach to Global-Stability Problems. *SIAM J. Math. Anal.* **1996**, *27*, 1070–1083. [[CrossRef](#)]
59. Feng, X.M.; Ruan, S.G.; Teng, Z. D.; Wang, K. Stability and backward bifurcation in a malaria transmission model with applications to the control of malaria in China. *Math. Biosci.* **2015**, *266*, 52–64. [[CrossRef](#)] [[PubMed](#)]
60. Zhou, F.; Yu, T.; Du, R.H.; Fan, G.; Liu, Y.; Liu, Z.; Xiang, J.; Wang, Y.; Song, B.; Gu, X.; et al. Clinical course and risk factors for mortality of adult inpatients with COVID-19 in Wuhan, China: A retrospective cohort study. *Lancet* **2020**, *395*, 1054–1062. [[CrossRef](#)] [[PubMed](#)]
61. Long, Q.X.; Tang, X.J.; Shi, Q.L.; Li, Q.; Deng, H.J.; Yuan, J.; Hu, J.L.; Xu, W.; Zhang, Y.; Lv, F.J.; et al. Clinical and immunological assessment of asymptomatic SARS-CoV-2 infections. *Nat. Med.* **2020**, *26*, 1200–1204. [[CrossRef](#)]
62. Covid-19 Coronavirus Pandemic. Available online: <https://www.worldometers.info/coronavirus/countries> (accessed on 14 August 2022).
63. Stephen, A.D. *Forecasting: Principles and Applications*; McGraw-Hill: New York, NY, USA, 1998.
64. Lewis, C.D. *Industrial and Business Forecasting Methods: A Practical Guide to Exponential Smoothing and Curve Fitting*; Butterworth-Heinemann: Oxford, UK, 1982.
65. Chitnis, N.; Hyman, J.M.; Cushing, J.M. Determining important parameters in the spread of malaria through the sensitivity analysis of a mathematical model. *Bull. Math. Biol.* **2008**, *70*, 1272–1296. [[CrossRef](#)]

Disclaimer/Publisher’s Note: The statements, opinions and data contained in all publications are solely those of the individual author(s) and contributor(s) and not of MDPI and/or the editor(s). MDPI and/or the editor(s) disclaim responsibility for any injury to people or property resulting from any ideas, methods, instructions or products referred to in the content.